

Performance evaluation of vehicular communication in terahertz band

Enis Körpe^{1,2}, Mustafa Alper Akkaş³, Radosveta Sokullu¹

The Terahertz (THz) band is seen as one of the potentially essential technologies to meet the data throughput requirements of terabits per second (Tbits) in future networks. Considering vehicular communication in particular, the current vehicular communication technologies cannot cope with the rapidly increasing data traffic. To deliver increased capacity and data rate with reduced latency, new technologies and methodologies are therefore required. It is recognized that one possible technology to meet these needs is THz technology. Since the change in distance between vehicles due to their speed affects THz communication, channel modeling was carried out for single-lane and multi-lane vehicular communication scenarios in this study. The system's performance was also examined. Performance metrics were determined as path loss, signal-to-noise ratio (SNR), capacity and bit error rate (BER). While performing these analyses, the absorption of THz waves is taken into account and the High-Resolution Transmission Molecular Absorption Database (HITRAN) was used to model it. As a result, the most appropriate circumstances for successful vehicular communication have been identified and studied.

Keywords: terahertz, vehicular communication, SNR, BER, HITRAN

1 Introduction

According to data traffic for the beyond-fifth generation (B5G) future, bandwidths less than 90 GHz will not be able to fulfill demand for data rates [1]. Terabits per second (Tbps) data rates will likely be needed by cellular and vehicle applications of the future. The Terahertz band (0.1-10 THz) is considered to be an advanced technology that can accommodate huge data rates because of this. THz band communication has thus received a lot of interest in the scientific community during the past 10 years. This interest is anticipated to persist as advancements in a number of fields, including electronic parts, channel modeling, and THz band standardization, continue to encourage more research activity [2, 3].

Applications like autonomous driving, self-parking, speed, and lane management have emerged as a result of the rise in the number of vehicles that wirelessly access to the internet and communicate with each other. Vehicle-to-Vehicle (V2V), Vehicle-to-Infrastructure (V2I) and Vehicle-to-Everything (V2X) communications show great potential for autonomous driving and connecting vehicles with 5G and beyond [4]. However, the spectrum resources of today's technology protocols such as Long-Term Evolution (LTE) and Dedicated Short-Range Communication (DSRC) are limited. Therefore, the THz band can be used in vehicular communications as it provides ultra-high data rate [5].

The capacity of the vehicles to wirelessly connect to the internet has sparked the development of new vehicular communication technologies. It is anticipated that as vehicular communication advances, each vehicle will be able to identify nearby vehicles and determine the current traffic condition using the data gathered by offering direct information exchange between vehicles. As a result, vehicles alert their drivers to potential threats like traffic accidents, road construction, and erroneous lane changes. Since exact information must be communicated in challenging and highly dynamic environmental conditions, communication must comply with the highest standards of quality.

The fundamental principle of vehicular communication is that each vehicle periodically transmits status information. These messages, also known as beacon messages, include data on the driver's current location, speed, acceleration, and direction of travel. Mutual awareness of vehicles is ensured via messages. To get correct awareness of the surrounding environment for vehicles near the transmitter in question, it is especially crucial that they receive beacon messages. Beacon signals have unique communication qualities that must be considered. Each vehicle first transmits beacon messages. Second, frequently updated information is sent out in beacon messages. Third, broadcasts are used to deliver messages because they do not have a designated receiver.

¹Department of Electrical and Electronics Engineering, Ege University, Izmir, Turkey

²Department of Electrical and Electronics Engineering, Alanya Alaaddin Keykubat University, Alanya, Turkey

³Department of Computer Engineering, Bolu Abant İzzet Baysal University, Bolu, Turkey

e-mail: enis.korpe92@gmail.com

As a result of THz waves' high data rate, high capacity, and short delay, it is thought that they can significantly improve vehicular communication. With the exception of metals and liquids, THz waves are generally unaffected by their surroundings. However, certain frequencies can cause the molecules of various materials to vibrate. THz waves can be absorbed more quickly as a result of this vibration, which affects the communication transmission path. Due to this, it's important to take into account how THz waves at specific frequencies are absorbed [6]. THz wave absorption loss can be calculated in a variety of ways. One of the most well-known is the High-Resolution Transmission Molecular Absorption Database (HITRAN).

1.1 High-resolution transmission molecular absorption database (HITRAN)

HITRAN is a crucial online tool for examining the absorption spectra of different atmospheric gases [7]. The instrument is based on the widely used Spectroscopy of Atmospheric Gases (SPECTRA) and HITRAN database of infrared spectrum spanning from microwave to ultraviolet and higher spectral areas [8]. The tool shows absorption coefficients while accounting for several factors including pressure, temperature, and latitude. The air's constituent elements differ in specific proportions. These percentages are categorized according to a set of rules. The IAO and USA standards are the most commonly utilized.

When analyzing the path loss, signal-to-noise ratio (SNR), capacity and bit error rate (BER) in the THz band for single-lane and multi-lane vehicular communications, the impacts of molecular absorption and reflection have been taken into consideration in this paper. We used HITRAN when modeling molecular absorption. This work has the following contributions:

- The path loss, SNR, capacity and BER performance of the THz band vehicular communication system is analyzed by taking into account both molecular absorption and reflection of THz waves.
- By creating different THz vehicular communication scenarios, the conditions under which vehicles can communicate successfully in these scenarios are determined and analyzed.
- The effects of the speed difference between vehicles on the system results are investigated and results are presented for specific cases.

This paper is organized as follows. An overview of the research on vehicular communication in the THz band that has been published in the literature is given in Section 2. Section 3 describes the electromagnetic modeling of THz waves for vehicular communication.

Section 4 presents and explains the path loss, SNR, capacity, and BER results for single-lane and multi-lane vehicular communication. Following a summary of the study's findings, recommendations for further research are made.

2 Related works

There are various studies in the literature regarding Terahertz band vehicular communication. In [1], the performance of the generalized hybrid beamforming (HBF) array structure using the THz channel model was investigated in a scenario involving pedestrians and vehicle users. Simulation findings show that the overlapping subarray implementation maintains a balance in terms of spectrum efficiency, energy efficiency, and hardware cost when compared to common fully-linked and sub-linked designs. Path loss, signal-to-noise ratio (SNR), and capacity analyses were not applied and the investigations were restricted to single-lane vehicular communication. In [9], wave propagation in 300 GHz single-lane and multi-lane vehicular communication scenarios was examined. With the measurement data obtained, mathematical approaches characterizing the low THz band channel properties for each scenario were derived. Measurement data are determined as path loss and path gain. While making the analyses, it was not taken into account that THz waves were absorbed, and absorption loss was not mentioned in the mathematical expressions. The effects of multipath interference and beam direction error on THz band vehicular communications were investigated in [10]. The system's performance in terms of failure probability was evaluated when multipath, misalignment, and pointing problems were present. Numerical results show that the THz connection degrades rapidly and severely at higher speeds when the signal-to-interference-plus-noise ratio (SINR) is below a pre-defined threshold. High antenna gain, antenna arrays, or multiple-input multiple-output (MIMO) antennas are not taken into account in this study. Similar to the previous study, no mathematical modeling of absorption loss was carried out. In [11], the path loss and Rician K-factor of the vehicle-to-infrastructure (V2I) channel were investigated under sunny, rainy and snowy weather conditions. The results show that rain and snow have a significant impact on the path loss of the system. However, no analysis has been made about the capacity and SNR performance of the channel. Absorption loss was not taken into account. In the study [12], utilizing measurements of 300 GHz propagation in vehicle-to-vehicle (V2V) systems and IEEE 802.15.3d parameters, a mathematical framework for comparing multi-hop transmission systems with various antenna placements was constructed. Performance parameters included coverage, base station (BS) availability, and data rate. The findings indicate that, despite having a much lower

data rate, the windshield placement is more favorable since it is less vulnerable to the rate of technology penetration and generally has far wider coverage. In the study [13], interference from side lanes for low terahertz bands was investigated utilizing simulation and analytical approaches in two different situations, including highway and urban road environments. The findings demonstrate that using two-dimensional stochastic models, interference from side lanes may be accurately predicted. In [14], the ray tracing approach is used to investigate the V2I channel in a typical urban environment at 110 GHz. The channel's path loss, time of arrival (ToA), and direction of arrival (DoA) were examined. However, the absorption of THz waves was not taken into account when performing path loss analysis. The results of the simulations demonstrate that the channel model developed is a reliable representation of the urban V2I scenario in the low THz band. [15] depicts a small cell base station in a downlink heterogeneous THz network. For both cellular and vehicle user devices, research was done into the optimal power distribution and SINR. The numerical results show that THz communication works well in terms of data rates, but that bit error rate (BER) performance suffers as a result of vehicle speed.

Considering the studies examined in the literature, it is observed that molecular absorption is often not taken into account when analyzing path loss. Additionally, most studies have not examined the conditions under which vehicles can communicate successfully. This work therefore concentrated on investigating various scenarios involving the effects of molecular absorption as well as reflection on path loss in the THz band. By performing SNR analysis in different vehicular communication scenarios, we determined the conditions under which vehicles can communicate successfully. Consequently, our work's primary contributions are reflections that consider the specifics of THz propagation, path loss, SNR, capacity, and BER analyses for the THz band under a range of temperature, pressure, seasonal variations, and geographic locations.

3 Electromagnetic modeling of THz waves for different vehicular communication scenarios

To effectively conduct THz band studies and develop products that are ready for the market, communication channel characteristics need to be modeled and investigated for different environments and gas compositions. These analyses require electromagnetic modeling of THz waves. Modeling of THz waves was based on the Friss equation shown below.

$$P_r = P_t + G_t + G_r - L_f \quad (\text{dB}) \quad (1)$$

In this equation, P_t stands for transmitting power, G_r and G_t are receiver and transmitter gains and L_f is the free-space path loss given as

$$L_f(f, d) = 20 \log_{10} \frac{4\pi f d}{c} \quad (\text{dB}) \quad (2)$$

In Eqn. (2), f is the operating frequency (Hz), d is the distance between the transmitter and the receiver (m) and c is the speed of light ($c=3 \times 10^8$ m/s).

However, in addition to the free-space path loss, the absorption loss also needs to be considered in THz medium communication. Theoretically derived representation of the absorption loss is [16]

$$L_{abs}(f, d) = k(f)_{gas} d 10 \log_{10} e \quad (\text{dB}) \quad (3)$$

In Eqn. (3), d represents the distance (m) between the transmitter and the receiver, and $k(f)_{gas}$ is the gaseous medium frequency-dependent absorption coefficient. For the value of this coefficient, the High-resolution Transmission Molecular Absorption Database (HITRAN) was used. Table 1 shows the used HITRAN parameters.

Table 1. HITRAN parameters used for this study

Model Used: IAO Model, Middle Latitudes, Summer Season, H=0 Minimum Wave Number: WNmin= 0 cm ⁻¹ Maximum Wave Number: WNmax= 33.36 cm ⁻¹ Temperature: T= 296 K Pressure: P= 1 atm

In HITRAN, the absorption coefficient's spectral dependence $k(w)$ is calculated by line-by-line method which is given as

$$k(w) = N(p, T) \times \sum_{i=1}^q n^i \sum_{j=1}^{s(i)} I^{(ij)}(T) \phi(w, w^{(ij)} - w^{(ij)} + w; p, T) \quad (4)$$

In Eqn (4), $N(p, T)$ is the concentration of molecules, p is pressure, k is the Boltzmann constant and T is temperature. $I^{(ij)}$ is the j^{th} line's integral intensity for the i^{th} isotopic species, $\phi^{(ij)}$ is the line shape of the j^{th} line, n^i is the mixing ratio of the i^{th} isotopic species, $w^{(ij)}$ is the j^{th} line's center position and w is the vacuum wavenumber of radiation.

Based on the equations presented above, we proceed with the two vehicular scenarios that were outlined below.

3.1 Scenario 1: Single-lane vehicular communication with line-of-sight propagation

In the first scenario, which can be seen in Fig. 1, vehicles are travelling in a single lane and there is only a line-of-sight (LoS) path between them.

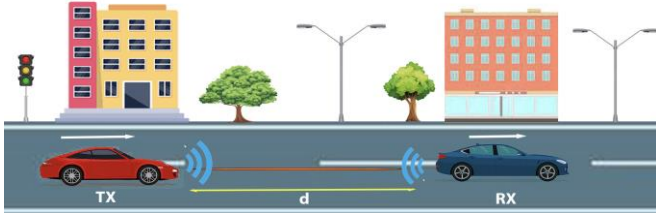


Fig. 1. Single-lane vehicular communication with LoS propagation

For this scenario, Eqns. (5) and (6) provide the system's total path loss and signal-to-noise ratio (SNR).

$$L_{one} = L_f + L_{abs} \quad (\text{dB}) \quad (5)$$

$$\text{SNR} = P_t - L_{one} - P_{noise} \quad (\text{dB}) \quad (6)$$

In Eqn. (6), P_t represents transmitter's power, L_{one} represents the one-path total path loss and P_{noise} is the noise power calculated by a formula-of-practice $P_{noise}(\text{dBm}) = 10 \log_{10} P(\text{W}) + 30$. Power P (entered in watts) is given by the product $k.T.B$. Here, temperature $T=296$ K, k is the Boltzmann constant, and B is the frequency bandwidth in Hz. dBm stands for decibel-milliwatts. It is a dimensionless unit used to measure the power level with reference to 1 milliwatt. Thus, the power level of 0 dBm represents 1 milliwatt.

Capacity and BER of the system are given in Eqns. (7) and (8).

$$C = \sum_i \Delta f \log_2 \left(1 + \frac{P_t}{L_{one}(f_i, d) \cdot P_{noise}(f_i, d)} \right) \quad (7)$$

$$P_b = 0.5 \cdot \text{erfc} \left(\sqrt{\frac{P_t}{L_{one}(f, d) \cdot P_{noise}(f, d)}} \right) \quad (8)$$

3.2 Scenario 2: Multi-lane vehicular communication

In the second scenario as shown in Fig. 2, vehicles are moving in a multi-lane and we consider ground-surface reflection and vehicle-vehicle reflection. Therefore, two reflected paths (NLoS paths) and one direct ray (LoS path) create three-ray propagation. According to this scenario, the total path loss is given as

$$L_{three} = L_d + L_s + L_t \quad (\text{dB}) \quad (9)$$

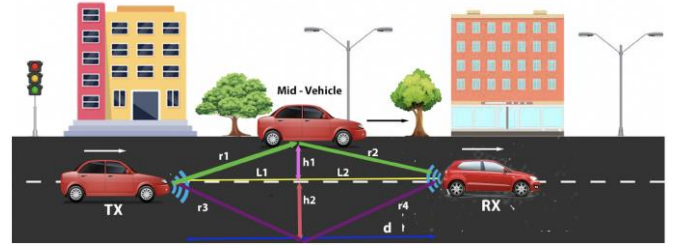


Fig. 2. Multi-lane vehicular communication

In Eqn. (9), L_{three} represents the three-path total path loss, $L_d = L_f + L_{abs}$ is direct path loss, $L_s = -V_s$ is the reflection loss due to the second path and $L_t = -V_t$ is the reflection loss due to the third path. V_s and V_t are expressed in Eqns. (10) and (11) [17, 18].

$$V_s^2 = 1 + \left(R_s \times \exp(-\alpha \Delta_s(r)) \right)^2 - 2 \times R_s \exp(-\alpha \Delta_s(r)) \times \cos \left(\pi - \left(\varnothing_s - \frac{2\pi}{\lambda} \Delta_s(r) \right) \right) \quad (10)$$

$$V_t^2 = 1 + \left(R_t \times \exp(-\alpha \Delta_t(r)) \right)^2 - 2 \times R_t \exp(-\alpha \Delta_t(r)) \times \cos \left(\pi - \left(\varnothing_t - \frac{2\pi}{\lambda} \Delta_t(r) \right) \right) \quad (11)$$

In Eqn. (10), for the second path, \varnothing_s is phase angle of the reflection coefficient, R_s is amplitude of the reflection coefficient, and α is the attenuation constant. λ is the medium's wavelength and $\Delta_s(r) = r_3 + r_4 - d$ is the difference of reflected and direct rays. For three-ray propagation in THz vehicular communication, α , the attenuation constant can be thought of as absorption coefficient $k(f)_{gas}$. The reflection coefficient, Γ_s is given in Eqn. (12) [19].

$$\Gamma_s = \frac{n_t \cos \theta_i - n_i \cos \theta_r}{n_i \cos \theta_r + n_t \cos \theta_i} \quad (12)$$

In Eqn. (12), n_i represents the refractive index of the incident medium (air), n_t represents the refractive index of the transmitted medium (asphalt), θ_i and θ_r represent the incident angle and refracted angle, respectively. ($\sin \theta_i = \frac{L_1}{r_3}$ and $\sin \theta_r = \frac{n_i}{n_t} \cdot \sin \theta_i$)

In Eqn. (11), for the third path, \varnothing_t is the phase angle of the reflection coefficient, R_t is the amplitude of the reflection coefficient, and α is the attenuation constant. λ is the medium's wavelength and $\Delta_t(r) = r_1 + r_2 - d$ is the difference of reflected and direct rays. For three-ray propagation in THz vehicular communication, α , the attenuation constant can be thought of as absorption coefficient $k(f)_{gas}$. The reflection coefficient, Γ_t is given as [19]

$$\Gamma_t = \frac{n_t \cos \theta_i - n_i \cos \theta_r}{n_i \cos \theta_r + n_t \cos \theta_i} \quad (13)$$

In Eqn. (13), n_i represents the refractive index of the incident medium (air), n_t represents the refractive index of the transmitted medium (vehicle), θ_i and θ_r represent the incident angle and refracted angle, respectively. ($\sin \theta_i = L_1/r_1$ and $\sin \theta_r = \frac{n_i}{n_t} \cdot \sin \theta_i$)

SNR, capacity and BER expressions of the systems are given in Eqns. (13) to (16).

$$SNR = \frac{P_t}{L_{three}(f, d) \cdot P_{noise}(f, d)} \quad (14)$$

$$C = \sum_i \Delta f \times \log_2 \left(1 + \frac{P_t}{L_{three}(f_i, d) \cdot P_{noise}(f_i, d)} \right) \quad (15)$$

$$P_b = 0.5 \times \left(1 - \sqrt{\frac{SNR}{1+SNR}} \right) \quad (16)$$

In the next section, we present path loss, SNR, capacity and BER analyses of the single-lane and multi-lane vehicular communication systems using the equations we have derived in Section 3.

4 Case study

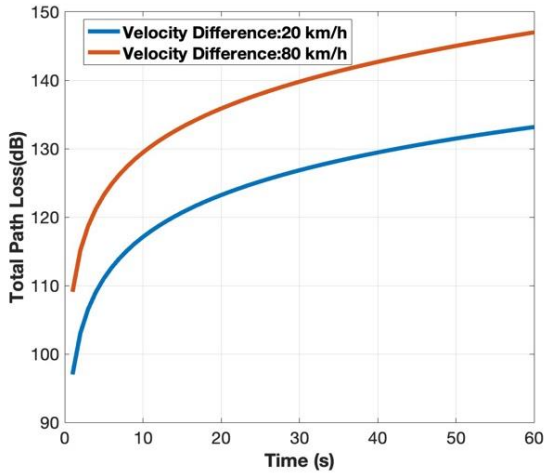
In this study, two different case scenarios were determined and we analyzed the system for these scenarios. The simulations were done using MATLAB environment.

4.1 Performance of the system in Scenario 1

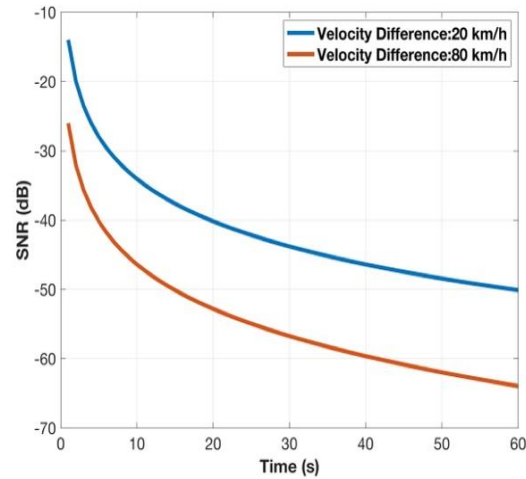
The system in scenario 1 has been tested with vehicles moving at speed differences 20 km/h and 80 km/h. Urban traffic may be thought of as a scenario where there is a 20 km/h speed difference between the vehicles, while highway traffic can be thought of as a scenario where there is an 80 km/h speed difference. THz horn antennas are used as transmitting and receiving antennas. Horn antennas are antennas which are created to operate in the THz band, with a gain between 20 dB and 30 dB [20]. These antennas are located in the headlights of the vehicles. The distance between the vehicles was 0 m at the beginning, and the total path loss, signal-to-noise ratio (SNR), capacity and BER performances of the system were examined in the first 60 second period. The simulation parameters and values used are illustrated in Tab. 2. The simulation results are demonstrated in Figs. 3a to 3d.

Table 2. Simulation parameters for Scenario 1

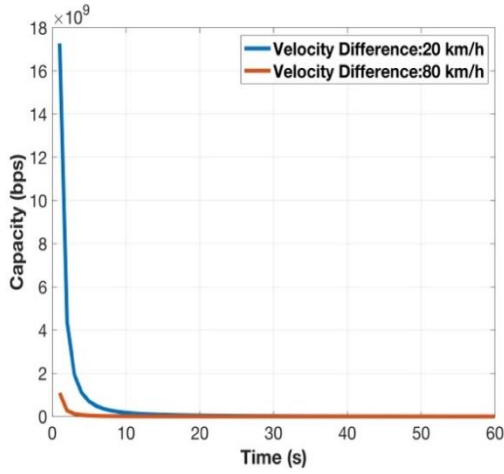
Simulation parameters
Transmitting Power: 24 dBm
Antenna Gain: 30 dBi
Operating Frequency: 0.3 THz
Modulation Type: Binary Phase Shift Keying (BPSK)
Channel Model: Additive White Gaussian Noise (AWGN)



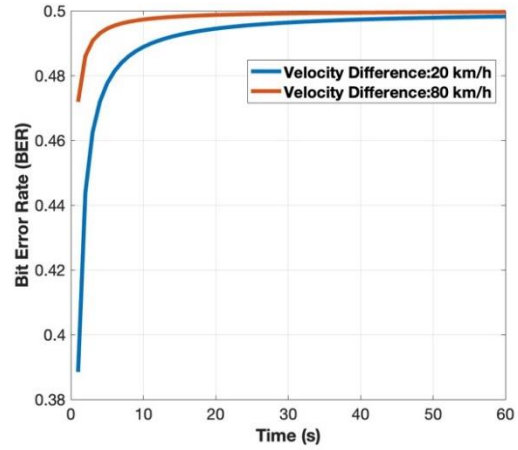
(a) Total path loss of the system for scenario 1 in 60 second period



(b) SNR of the system for scenario 1 in 60 second period



(c) Capacity of the system for scenario 1 in 60 second period



(d) BER of the system for scenario 1 in 60 second period

Fig. 3. Simulation results of the system for scenario 1 in 60 second period

In Fig. 4, the variation of the system’s total path loss according to the speed difference between the vehicles and the time is shown in three dimensions. The regions above the maximum tolerable path loss for successful communication are shown in red. Mathematical formula for the maximum tolerable path loss is shown in Eqn. (17).

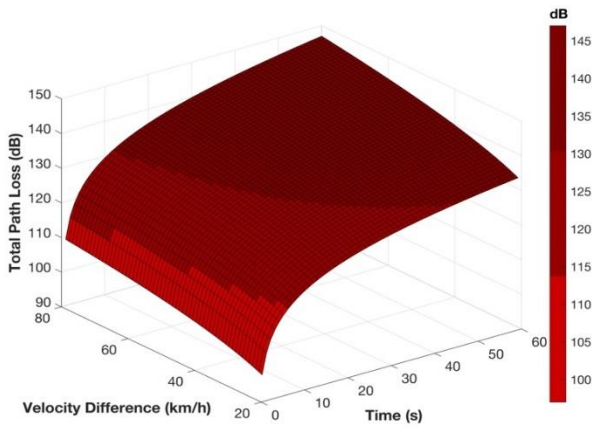


Fig. 4. Total path loss of the system for scenario 1 in 60 second period (three-dimensional)

$$L_{max} = P_t - SNR_T - P_{noise} \quad (\text{dB}) \quad (17)$$

In Equation 18, $SNR_T(\text{dB})$ represents the minimum SNR (12 dB) required for successful communication. The maximum tolerable path loss was found to be 71 dB by calculations using this equation. Path loss results obtained in this scenario are above the maximum tolerable path loss values.

$$SNR = P_t + G_t + G_r - L_{onpath} - P_{noise} \quad (\text{dB}) \quad (18)$$

When Figs. 3(b) to 3(d) are examined, it is observed that the SNR values of the system are low and therefore the BER is high resulting in low capacity performance of the system. Under these conditions, successful communication between vehicles cannot be achieved. For this reason, after finding the SNR values, link budget analysis should be performed in order to find out under which conditions a successful communication can occur [21]. With the link budget analysis, the SNR of the system can be found as in Eqn. (18).

Figure 5 shows the SNR performance of the system after the link budget analysis.

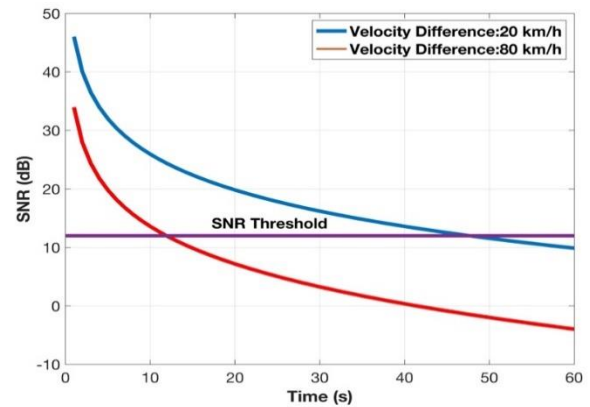


Fig. 5. SNR of the system for scenario 1 in 60 second period after link budget analysis

It is observed that as the speed difference between vehicles increases, the time they can stay in connection decreases. The limit SNR value for successful communication is 12 dB. As a result, for two vehicles traveling at a speed difference of 20 km/h, a successful communication is not possible after $t=48$ s. For an

80 km/h speed difference, this time is $t=12$ s. Figure 6 shows the variation of the total path loss of the system according to the speed difference and time between the vehicles, in three dimensions, after the link budget analysis.

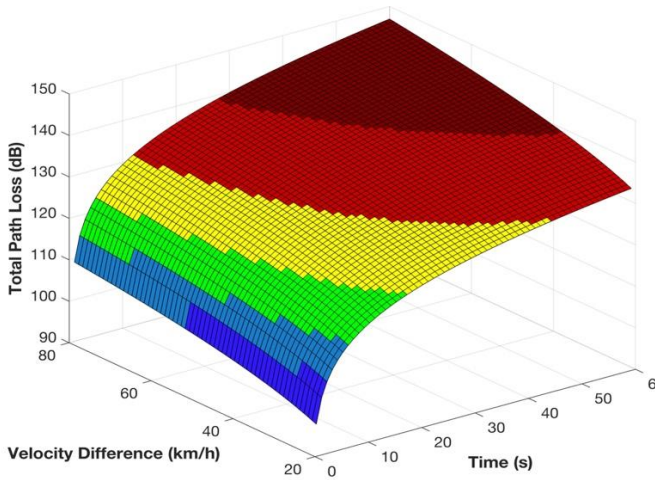


Fig. 6. Total path loss of the system after link budget analysis for scenario 1 in 60 second period (three-dimensional)

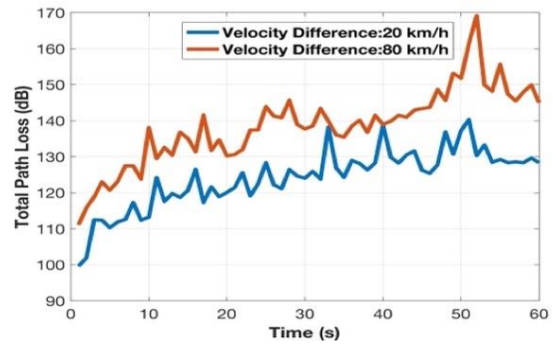
Considering the link budget analysis, the maximum tolerable path loss is given in Eqn. (19).

$$L_{max} = P_t + G_t + G_r - SNR_T - P_{noise} \quad (\text{dB}) \quad (19)$$

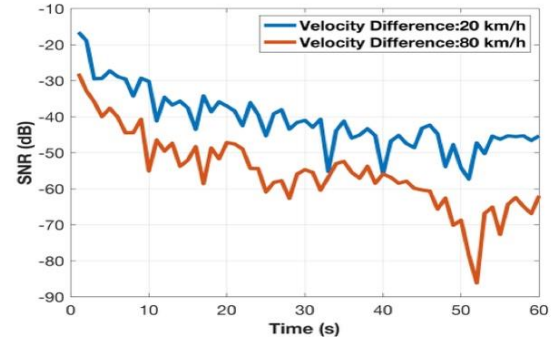
The maximum tolerable path loss was found to be 131 dB by calculations using this equation. In Fig. 6, the regions where successful communication can be achieved are shown in blue, green and yellow colors, and the regions where successful communication is not possible are shown in red. The results obtained coincide with the results in Fig. 5.

4.2 Performance of the system in Scenario 2

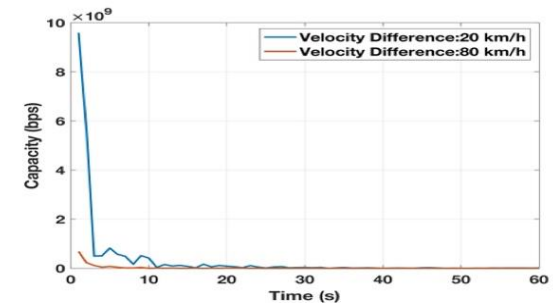
This system has been tested for the speed difference between the transmitting and receiving vehicles of 20 km/h and 80 km/h. Vehicles are traveling at different speeds. The initial distance between the transmitter and receiver vehicles was 5.5 m, and the path loss, SNR, capacity and BER performance of the system were examined in the first 60 s period. The simulation parameters and values used are given in Tab. 3. The simulation findings are demonstrated in Figs. 7a to 7d.



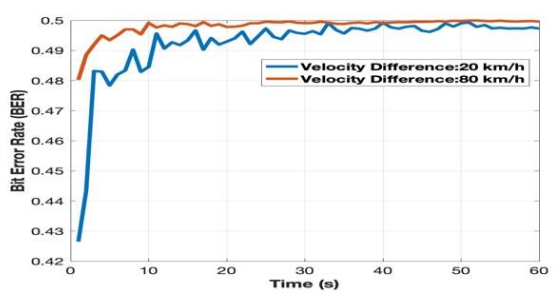
(a) Total path loss of the system for scenario 3 in 60 second period



(b) SNR of the system for scenario 3 in 60 second period



(c) Capacity of the system for scenario 3 in 60 second period



(d) BER of the system for scenario 3 in 60 second period

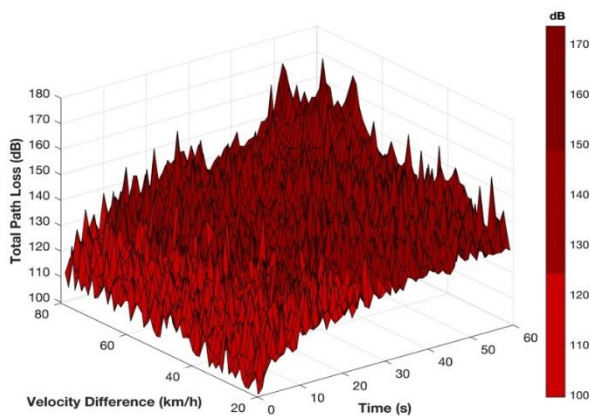
Fig. 7. Simulation results of the system for scenario 2 in 60 second period

Table 3. Simulation parameters for scenario 2

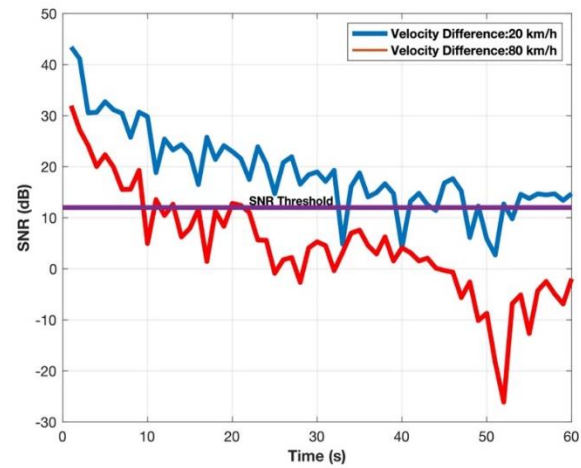
Simulation parameters
Transmitting Power: 24 dBm
Antenna Gain: 30 dBi
Operating Frequency: 0.3 THz
Height and Width of Vehicles: 1.5 m
Length of Vehicles: 3 m
Modulation Type: Binary Phase Shift Keying (BPSK)
Channel Model: Rayleigh Fading Channel

Investigating Figs. 7a to 7c reveals that the system's SNR values are inadequate which also affects the BER and capacity performance of the system. Successful vehicle-to-vehicle communication is impossible in these circumstances. For this reason, after finding the SNR values, link budget analysis should be done for this scenario, as was done in previous scenario in order to find out under which conditions a successful communication can occur.

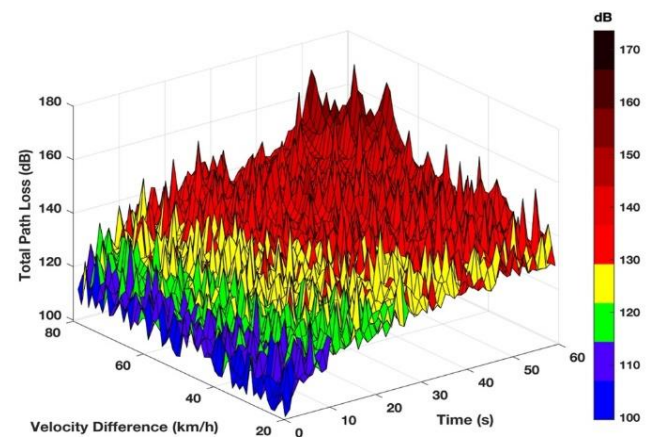
In Fig. 8, the change of the total path loss of the system according to the speed difference between vehicles and time is shown in three dimensions.

**Fig. 8.** Total path loss of the system for scenario 2 in 60 second period (three-dimensional)

In Fig. 8, the regions above the maximum tolerable path loss for successful communication are shown in red. Path loss results obtained in this scenario are above the maximum tolerable path loss results (71 dB). Figure 9 shows the SNR performance of the system after the link budget analysis.

**Fig. 9.** SNR of the system for scenario 2 in 60 second period after link budget analysis

One can see that the amount of time that two vehicles can remain connected decreases as the difference in speed between them increases. The limit SNR value for successful communication is 12 dB. Therefore, for two vehicles traveling at a speed difference of 20 km/h, the SNR started to fall below the threshold value at $t=32$ s. There is no successful communication between the vehicles $t=32-34$ s, $t=39-41$ s, $t=47-54$ s. For two vehicles traveling at a speed difference of 80 km/h, successful communication cannot be achieved after $t=10$ s. Figure 10 shows in three dimensions the change of the total path loss of the system according to the speed difference between vehicles and time after the link budget analysis is performed.

**Fig. 10.** Total path Loss of the system after link budget analysis for scenario 2 in 60 second period (three-dimensional)

In Fig. 10, the areas where successful communication may be obtained are depicted in blue, green, and yellow, while the areas where successful communication cannot be achieved are depicted in red. The outcomes are consistent with those shown in Fig. 9.

5 Conclusion

In this study, a detailed investigation was carried out for single-lane and multi-lane vehicular communication scenarios and analyses of path loss, signal-to-noise ratio (SNR), capacity and bit error rate (BER) were presented. An important contribution is that the possibility of THz signal absorption by air components like water vapor and oxygen was taken into consideration, which has not been done in previous studies. Absorption loss was thus also included in the path loss analysis. The absorption losses were computed using the High-Resolution Transmission Molecular Absorption Database (HITRAN). HITRAN has made it possible to perform path loss, SNR, capacity, and BER analyses for the THz band under a range of climatic, seasonal, and geographical conditions. As a result, HITRAN is a helpful tool for researching THz band vehicular communications. We considered reflection and absorption from the air and road surface environment in addition to the free space path loss when calculating the path loss. We also determined the circumstances in which vehicles can communicate successfully. We found that as the speed difference between vehicles increases, the time they can stay connected decreases. We observed that reflections from the road and vehicles increase the path loss of the system, thus reducing the time in which vehicles can communicate with each other successfully. For THz communication, absorption and reflection are crucial. For the purpose of developing a strong channel model for vehicular communication, such a thorough analysis is required. Modems in 6G communication are expected to be mounted on streetlights or roadside pontoons. As a result, further analysis using the techniques suggested in this paper for particular 6G modem applications will enable adjusting of modem parameters to accomplish outstanding performance.

References

- [1] S. A. Busari, K. M. S. Huq, S. Mumtaz, J. Rodriguez, Y. Fang, D. C. Sicker, S. Al-Rubaye, and A. Tsourdos, "Generalized hybrid beamforming for vehicular connectivity using THz massive MIMO," *IEEE Transactions on Vehicular Technology*, vol. 68, no. 9, pp. 8372–8383, 2019. doi:10.1109/TVT.2019.2921563.
- [2] I. F. Akyildiz, J. M. Jornet, and C. Han, "Terahertz band: Next frontier for wireless communications," *Physical Communication*, vol. 12, pp. 16–32, 2014. doi:10.1016/j.phycom.2014.01.006.
- [3] C. Lin, and G. Y. Li, "Energy-efficient design of indoor mmwave and sub-thz systems with antenna arrays," *IEEE Transactions on Wireless Communications*, vol. 15, no. 7, pp. 4660–4672, 2016. doi:10.1109/TWC.2016.2543733.
- [4] F. Arena, and G. Pau, "An overview of vehicular communications," *Future Internet*, vol. 11, no.2, pp. 1-12, 2019. doi:10.3390/fi11020027.
- [5] I. F. Akyildiz, J. M. Jornet and C. Han, "Teranets: ultra-broadband communication networks in the terahertz band," *IEEE Wireless Communications*, vol. 21, no. 4, pp. 130–135, 2014. doi:10.1109/MWC.2014.6882305.
- [6] A. Saeed, O. Gurbuz, and M. A. Akkas, "Terahertz communications at various atmospheric altitudes," *Physical Communication*, vol. 41, pp. 1-15, 2020. doi:10.1016/j.phycom.2020.101113.
- [7] I. E. Gordon, L. S. Rothman, R. J. Hargreaves, R. Hashemi, E. V. Karlovets, F. M. Skinner, et al., "The HITRAN2020 molecular spectroscopic database", *J. Quant. Spectrosc. Radiat. Transfer* 277, 107949, 2022. doi:10.1016/j.jqsrt.2021.107949.
- [8] C. N. Mikhailenko, Yu. L. Babikov, V.F. Golovko, "Information-calculating system spectroscopy of atmospheric gases. the structure and main functions," *Atmospheric and Oceanic Optics*, vol. 18, no. 9, pp. 685–695, 2005.
- [9] J. M. Eckhardt, V. Petrov, D. Moltchanov, Y. Koucheryavy, and T. Kürner, "Channel measurements and modeling for low-terahertz band vehicular communications," *IEEE Journal on Selected Areas in Communications*, vol. 39, no. 6, pp. 1590–1603, 2021. doi:10.1109/JSAC.2021.3071843.
- [10] S. Sathe, and D. B. Rawat, "On the performance of terahertz communications for vehicular wireless networks," *2022 IEEE International Conference on Communications Workshops (ICC Workshops)*, pp. 1–6, 2022. doi:10.1109/ICCWorkshops53468.2022.9882173.
- [11] H. Yi, K. Guan, D. He, B. Ai, J. Dou, and J. Kim, "Characterization for the vehicle-to-infrastructure channel in urban and highway scenarios at the terahertz band," *IEEE Access*, vol. 7, pp. 166984–166996, 2019. doi:10.1109/ACCESS.2019.2953890.
- [12] D. Moltchanov, V. A. Beschastnyi, D. Ostrikova, Y. Gaidamaka, Y. Koucheryavy, and K. E. Samouylov, "Optimal antenna locations for coverage extension in sub-terahertz vehicle-to-vehicle communications," *IEEE Transactions on Wireless Communications*, vol. 22, no. 9, pp. 5990–6002, 2023. doi:10.1109/TWC.2023.3238881.
- [13] V. Petrov, J. Kokkonen, D. Moltchanov, J. Lehtomaki, M. Juntti, and Y. Koucheryavy, "The impact of interference from the side lanes on mmwave/thz band v2v communication systems with directional antennas," *IEEE Transactions on Vehicular Technology*, vol. 67, no. 6, pp. 5028–5041, 2018. doi:10.1109/TVT.2018.2799564.
- [14] Y. Chen and C. Han, "Time-varying channel modeling for low-terahertz urban vehicle-to-infrastructure communications," *2019 IEEE Global Communications Conference (GLOBECOM)*, pp. 1–6, 2019. doi:10.1109/GLOBECOM38437.2019.9013865.
- [15] S. H. A. Samy, E. A. Maher, A. El-Mahdy and F. Dressler, "Power optimization of thz band heterogeneous vehicular networks," *2021 IEEE Vehicular Networking Conference (VNC)*, pp. 107–114, 2021. doi:10.1109/VNC52810.2021.9644672.
- [16] C. Han, A. O. Bicen, and I. F. Akyildiz, "Multi-ray channel modeling and wideband characterization for wireless communications in the terahertz band," *IEEE Transactions on Wireless Communications*, vol. 14, no. 5, pp. 2402–2412, 2015. doi:10.1109/TWC.2014.2386335.

- [17] M. A. Akkas, "Using wireless underground sensor networks for mine and miner safety," *Wireless Networks*, vol. 24, pp. 17–26, 2018. doi:10.1007/s11276-016-1313-0.
- [18] M. C. Vuran and I. F. Akyildiz, "Channel model and analysis for wireless underground sensor networks in soil medium," *Physical Communication*, vol. 3, no. 4, pp. 245–254, 2010. doi:10.1016/j.phycom.2010.07.001.
- [19] X. Dong and M. C. Vuran, "A channel model for wireless underground sensor networks using lateral waves," *2011 IEEE Global Telecommunications Conference - GLOBECOM 2011*, pp. 1–6, 2011. doi:10.1109/GLOCOM.2011.6134437.
- [21] Y. He, Y. Chen, L. Zhang, S.-W. Wong and Z. N. Chen, "An overview of terahertz antennas," *China Communications*, vol. 17, no. 7, pp. 124–165, 2020. doi:10.23919/J.CC.2020.07.011.
- [22] S. Haykin and M. Moher, *Modern Wireless Communication*, Prentice-Hall, Inc., USA, 2004.

Received 22 May 2024
